ACS Chemical Neuroscience

Research Article

pubs.acs.org/chemneuro

The Tachykinin Peptide Neurokinin B Binds Copper Forming an Unusual [$Cu^{II}(NKB)_2$] Complex and Inhibits Copper Uptake into 1321N1 Astrocytoma Cells

Debora Russino,[†] Elle McDonald,[†] Leila Hejazi,[‡] Graeme R. Hanson,[§] and Christopher E. Jones*[,†]

[†]The School of Science and Health, The University of Western Sydney, Locked bag 1797, Penrith, New South Wales 2759, Australia

[‡]Mass Spectroscopy Laboratory, The University of Western Sydney, Locked bag 1797, Penrith, New South Wales 2759, Australia

[§]Centre for Advanced Imaging, The University of Queensland, Brisbane, Queensland 4072, Australia

Supporting Information

ABSTRACT: Neurokinin B (NKB) is a member of the tachykinin family of neuropeptides that have neuroinflammatory, neuroimmunological, and neuroprotective functions. In a neuroprotective role, tachykinins can help protect cells against the neurotoxic processes observed in Alzheimer's disease. A change in copper homeostasis is a clear feature of Alzheimer's disease, and the dysregulation may be a contributory factor in toxicity. Copper has recently been shown to interact with neurokinin A and neuropeptide γ and can lead to generation of reactive oxygen species and peptide degradation, which suggests that copper may have a place in tachykinin function and potentially misfunction. To explore this, we have utilized a range of spectroscopic techniques to show that NKB, but not substance P, can bind Cu^{II} in an unusual [$Cu^{II}(NKB)_2$] neutral complex that utilizes two N-terminal amine and two imidazole nitrogen ligands (from each molecule of NKB) and the binding substantially alters the structure of the peptide. Using 1321N1 astrocytoma cells, we show that copper can enter the cells and subsequently open plasma membrane calcium channels but when bound to neurokinin B copper ion uptake is inhibited. This data suggests a novel role for neurokinin B in protecting cells against copper-induced calcium changes and implicates the peptide in synaptic copper homeostasis.

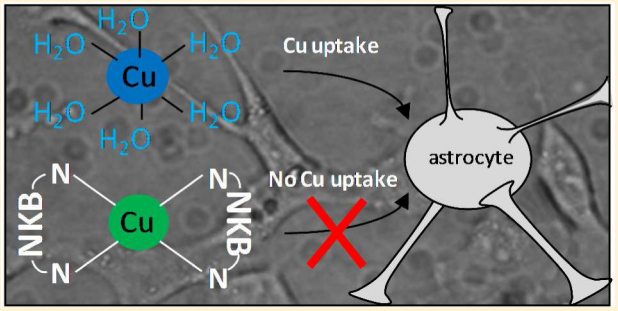

KEYWORDS: *Neurokinin B, tachykinin, copper, calcium, neurodegeneration, substance P, Fura2, EPR*

Neurokinin B (NKB, neuromedin K) is a 10 residue peptide that belongs to the tachykinin family of neuropeptides. Other members include the mammalian peptides substance P (SP), neurokinin A (NKA), the N-terminally extended forms of NKA neuropeptide K and neuropeptide γ, and hemokinin.[1] The family is characterized by the presence of a common C-terminal sequence FxGLM-NH_2, which is thought to be important for receptor binding and activation.[2] The biological activity of the tachykinin peptides lies with their ability to bind to G protein-coupled receptors and to mediate intracellular calcium release via several signaling pathways, including a $G_{q/11}$-coupled pathway, which involves the downstream generation of the second messengers diacylglycerol and IP_3.[2,3] SP, NKA, and NKB bind to neurokinin receptors NK1-R, NK2-R, and NK3-R, and although each peptide can bind to all the receptors, each has a preference for a particular receptor. Thus SP has a preference for NK1-R, NKA for NK2-R, and NKB for NK3-R. The structure of the peptides bound to their receptors is unclear; however, a recent modeling study looking at the interaction of NKB with NK3-R has highlighted not only how the C-terminal conserved domain directs receptor binding but also how the N-terminal residues may be involved in mediating receptor preference.[4]

Functionally, the tachykinins are involved in a diverse range of cellular signaling processes including roles in neuroprotection, neuroinflammation, and neurotrophic pathways.[1,2,5]

Much of our understanding of tachykinin function is due to research on the first member identified, SP, and the roles of NKA and NKB have remained more elusive. Recently though, NKB has been identified as a key molecule in normal reproductive function.[6,7] The tachykinins and their receptors are predominantly expressed in the central nervous system (CNS), although they do have peripheral nervous system (PNS) expression and are observed in other organs.[2,8] Of the main mammalian peptides, SP has both CNS and PNS expression, NKB is almost exclusively found in the CNS,[9] and NKA is largely expressed in the PNS. In the CNS, SP, NKB, and their receptors are highly expressed in regions of the brain that are important for cognition and emotion,[10,11] and

Received: April 29, 2013
Accepted: July 22, 2013
Published: July 22, 2013

   dx.doi.org/10.1021/cn4000988 | ACS Chem. Neurosci. 2013, 4, 1371−1381

antagonists for NK3-R are currently being pursued as therapeutics in a range of disorders including schizophrenia.[12,13]

The tachykinins have a well-documented involvement in several neurodegenerative disorders, particularly Alzheimer's disease (AD);[2] for example, AD patients appear to have diminished SP expression,[14] and there is also evidence that NKB has a role. Studies have shown that both NKB and SP appear to be able to protect neurons against the toxic effects of Aβ peptides.[15−18] More recently, NKB was shown to be able to protect neurons by acting as an antioxidant.[17] Further, the tachykinin peptides are also thought to be able to coassemble with Aβ peptides in the formation of amyloid fibrils, which may reduce neurotoxicity.[19] Nevertheless, the molecular mechanisms whereby tachykinin peptides limit Aβ toxicity and the relationship to AD remain unresolved.

One feature of AD, which is also common to other amyloidogenic disorders such as Parkinson's disease and prion disorders, is the dysregulation of metal ions, particularly copper, zinc, and iron.[20,21] In AD plaques, high concentrations of copper and zinc are found, and both are able to promote aggregation of Aβ peptides. Both metals are able to bind to monomeric Aβ peptides[22−26] as well as Aβ fibrils.[27] Copper is known to be released from neurons during normal activity,[28,29] where it may have a role in regulating synaptic function.[30] It is thought that the amyloid plaques formed in AD act as a "sink" leading to copper deficiency in neurons, and therapies aimed at stabilizing and normalizing neuronal copper concentrations appear to have been affective in improving cognitive decline in mouse models of AD.[31] An intriguing link between the tachykinins and metal ions is shown by the ability of NKA and neuropeptide γ to bind copper.[32,33] Both peptides also underwent oxidative cleavage in the presence of copper and hydrogen peroxide leading to loss of functional peptide, which for NKA was hypothesized to contribute to AD symptoms. No other tachykinins have been investigated for their copper binding properties, but inspection of the sequences of the mammalian tachykinins highlights the presence of a histidine residue at position 3 in NKB (DMHDFFVGLM-NH_2). The presence of a histidine at position 3 in proteins and peptides is common in copper-binding proteins and is known as an amino-terminal copper and nickel (ATCUN) binding site.[34] This site is observed, for example, in serum albumin[35] and binds copper via the histidine imidazole nitrogen, the histidine amide nitrogen, and the amino-terminal nitrogen. Depending on the pH, the fourth coordination site may be an amide nitrogen of residue 2 or a carbonyl oxygen. An ability to bind copper may not be restricted to human tachykinins as a recently identified zebra-fish NKB has a similar sequence, including the third position histidine, to human NKB.[36] Given the known independent involvement of copper and NKB in Alzheimer's disease, we hypothesized that the presence of an ATCUN motif implied the existence of a direct link between copper and NKB. We show here that NKB does indeed bind copper and the peptide can limit copper uptake into astrocytes.

RESULTS

Copper Binding to NKB. Initially, NKB was dissolved in 30 mM SDS, 10 mM n-EM at pH 7.6. Incorporating SDS not only improves solubility of this hydrophobic peptide but also mimics the lipid environment with which NKB is predicted to interact prior to binding to the receptor; indeed previous NKB structural investigations have been performed in a similar solvent.[37,38] To assess the binding of Cu^{II} to NKB, we initially utilized circular dichroism (CD) in the visible region. When $Cu^{II}Cl_2$ is added to NKB at pH 7.6, a chiral Cu^{II} center is formed with positive (490 nm) and negative (570 nm) bands in the CD titration (Figure 1A), as often observed in copper−amino acid complexes.[39] These bands increase in intensity until 0.5 equiv of Cu^{II} has been added (Figure 1C(■)). A similar titration is observed at higher pH (pH 8.7) (Figure 1B,C(▼)). The electronic absorption titrations at pH 7.9 (Figure 2A) and pH 8.9 (Figure 2B) show a similar behavior to the CD titration with a band at 520 nm increasing until 0.5 equiv has been added (inset, Figure 2A,B).[40] A similar stoichiometry was also obtained when the titration was performed in 10% DMSO/90% 10 mM nEM (data not shown). All of the optical titration data indicate the formation of a mononuclear copper center incorporating two molecules of NKB, that is, $[Cu^{II}(NKB)_2]$.

Interestingly, in both CD titrations (Figure 1A,B), an isodichroic point is observed at 520 nm corresponding to the λ_{max} in the electronic absorption spectrum (Figure 2), which does not change during the titration. The single, broad band observed in electronic spectroscopy is due to two or more overlapping d−d transitions, which CD can resolve, especially, as in this case, when the transitions result in CD signals of opposite sign.[39,41] The presence of an isodichroic point in the titration indicates that there is a single Cu^{II} binding site.

Mass spectra of NKB in 30 mM SDS, 10 mM n-EM at pH 7.5 show that NKB runs as a monomer ($[NKB + H]^+$, m/z 1210.54; calcd 1210.5) and a dimer ($[NKB_2 + H]^+$, m/z 2420.1; calcd 2420.0). The addition of copper at either 0.5 or 1.0 equiv results in the appearance of only a very small peak at m/z 2483.0, which is consistent with $[Cu^{II}(NKB)_2 + H]^+$, although the low intensity precludes accurate identification (data not shown). The lack of a reasonable copper-bound peak suggests that the complex either does not ionize well or is insufficiently stable to persist during the ionization process. However, lowering the ionization voltage from 40 to 20 V did not increase the intensity of the peak in the mass spectrum, which is in contrast to our previously reported studies with copper complexes of peptides and small molecules,[42−44] suggesting that the $[Cu^{II}(NKB)_2]$ complex is neutral and that it cannot be ionized.[45] This is consistent with the EPR results described below.

The formation of a 1:2 Cu/NKB complex is highly unusual for an ATCUN motif, which usually binds copper in a 1:1 stoichiometry, so we have undertaken a Cu^{II} binding titration of SP to see whether this is characteristic of tachykinins and, second, whether this unusual $[Cu^{II}(NKB)_2]$ center is observed for other metal ions, specifically Ni^{II}. Monitored by electronic spectroscopy, the addition of copper to SP in the same solvent as NKB (30 mM SDS, 10 mM nEM) resulted in the formation of a peak near 700 nm (not at 520 nm) in excess copper (Figure S1A, Supporting Information). Given that hydrated copper is usually observed near 800 nm, this peak most likely corresponds to Cu^{II} coordinated by water ligands and at least one nitrogen atom, likely the SP N-terminus. A Ni^{II} titration of NKB (Figure 3) shows a linear increase in absorbance at 420 nm until approximately 1.0 equiv of Ni^{II}, beyond which the slope changes (Figure 3, inset). Clearly, NKB, unlike SP, selectively binds Cu^{II} in an unusual binary complex involving two molecules of NKB, $[Cu^{II}(NKB)_2]$, which we show below is important for its biological function.

NKB Binds Copper through Four Nitrogen Ligands That Include Histidine 3. To help identify copper ligands, we

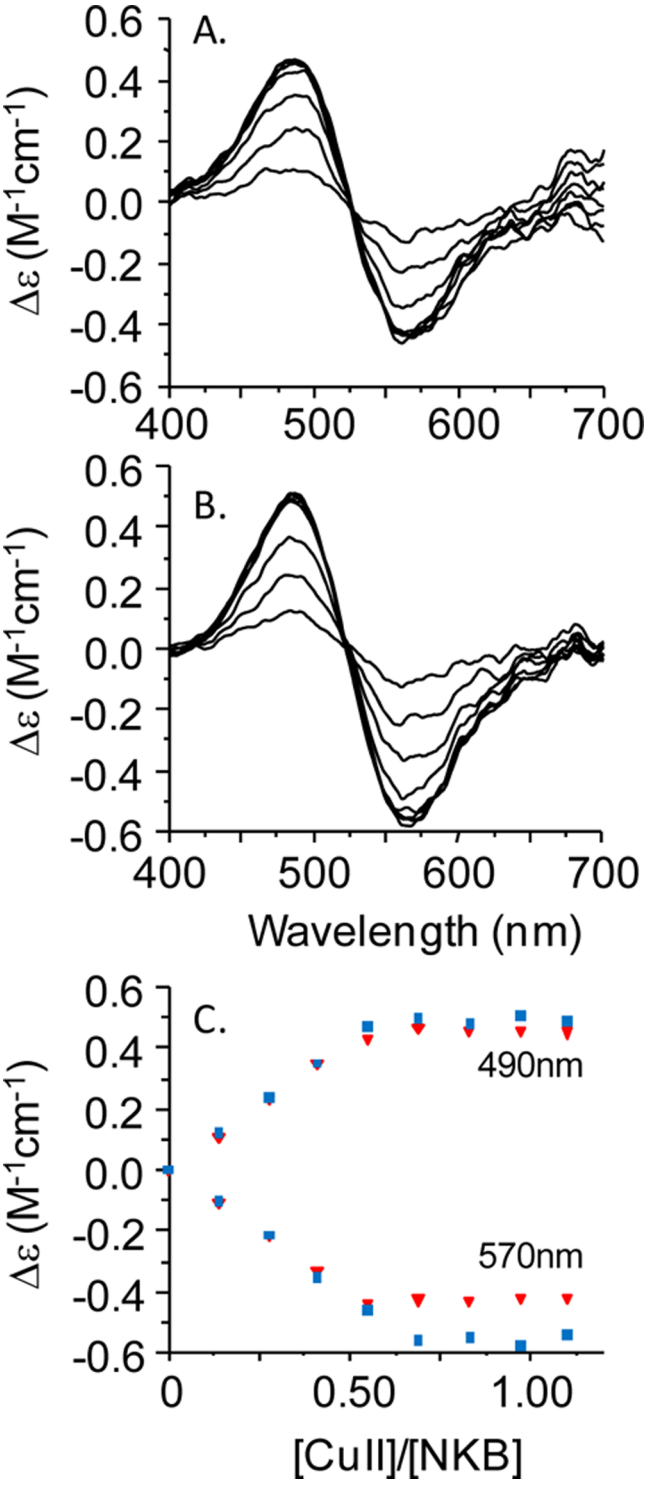

Figure 1. A Cu^{II} binding titration of NKB monitored by circular dichroism. (A) Titration of NKB (77.5 μM, 30 mM SDS, 10 mM nEM, pH 7.6) with $Cu^{II}Cl_2$ monitored between 400 and 700 nm. (B) Titration of NKB (77.5 μM, 30 mM SDS, 10 mM nEM, pH 8.7) with $Cu^{II}Cl_2$ monitored between 400 and 700 nm. (C) Molar ellipticity at 490 and 570 nm at pH 7.6 (■) and pH 8.7 (▼) plotted as a function of Cu^{II} equivalents highlights saturation at 0.5 equiv of Cu^{II}.

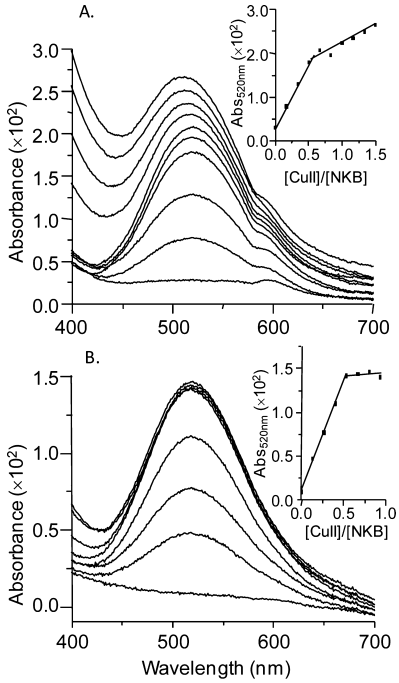

Figure 2. Cu^{II} binding titrations of NKB monitored by UV/vis spectroscopy. (A) NKB (108.5 μM) prepared in 30 mM SDS, 10 mM nEM, pH 7.9, was titrated with $CuCl_2$ and the absorbance in the visible region (400−700 nm) was monitored. (B) Copper titration of NKB (108.5 μM) prepared in 30 mM SDS, 10 mM nEM, pH 8.9. Insets show the absorbance at 520 nm plotted as a function of copper equivalents added ([Cu^{II}]/[NKB]), revealing a plateau in the binding curve at 0.5 equiv at both pH values.

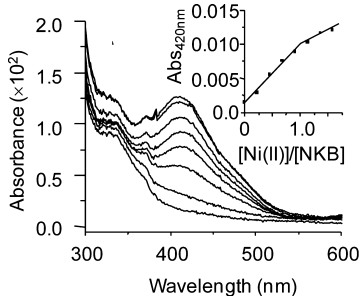

Figure 3. Ni^{II} binding titrations of NKB monitored by UV/vis spectroscopy. (A) NKB (108.5 μM) prepared in 30 mM SDS, 10 mM n-EM pH 8.9 was titrated with $NiCl_2$ and the absorbance between 300 and 600 nm was monitored. The inset shows the absorbance at 420 nm plotted as a function of copper equivalents added ([Ni^{II}]/[NKB]).

first utilized NMR. Cu^{II} is a metal ion that is paramagnetic irrespective of the coordination geometry (for mononuclear complexes) and leads to paramagnetic broadening and shifting of NMR peaks. However, these effects usually only occur over short distances (<7 Å), and if small amounts of Cu^{II} are added the broadening only affects the resonances from nuclei of ligands directly coordinated to the Cu^{II} ion. We obtained one-dimensional NMR spectra for apo-NKB and after the addition of 0.14 and 0.28 equiv of copper (Figure 4A−C). The identity of the peaks was determined from a TOCSY spectrum (τ_m = 75 ms) and compared with literature values.[37] Figure 4 shows that upon addition of Cu^{II} the peaks at 8.72 and 7.42 ppm broaden beyond detection. These peaks correspond to the C2H and C4H protons of the His3 imidazole side chain. There is a general broadening observed to most other peaks, largely due to the small size of the peptide (Figure 4; Figure S2, Supporting Information). We cannot discern amide proton changes

dx.doi.org/10.1021/cn4000988 | ACS Chem. Neurosci. 2013, 4, 1371−1381

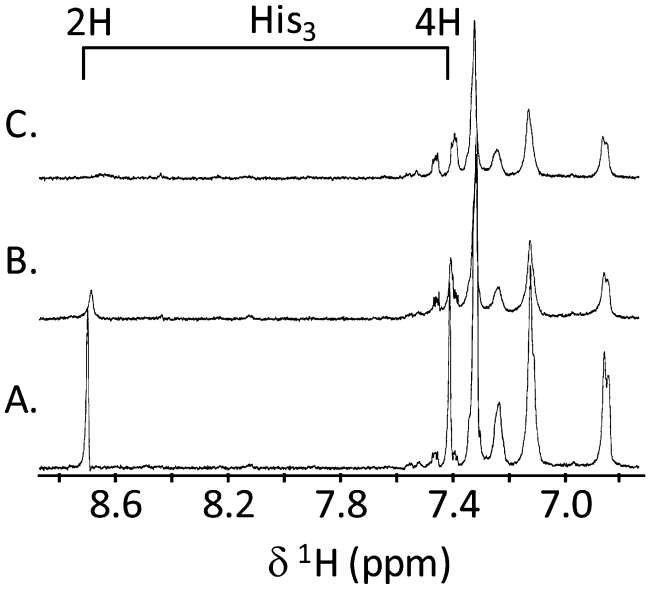

Figure 4. Cu^{II} titration of NKB (425 μM, 30 mM SDS-d_{25}, pH 7.6) monitored by NMR (500 MHz, 298 K). From bottom (A), spectrum of the aromatic and amide region of apo-NKB, (B) NKB after the addition of 0.05 equiv of $CuCl_2$ and (C) NKB after the addition of 0.2 equiv of $CuCl_2$. The chemical shift of the His3 imidazole 2H and 4H protons is shown.

because under these conditions amide protons are rapidly exchanging with the solvent and are not observed.

To further examine the coordination environment of the copper ion in NKB, we used EPR spectroscopy. The first derivative anisotropic frozen solution EPR spectrum (Figure 5a; Figure S3b, Supporting Information) of a solution containing Cu/NKB in the ratio of 1:2 in 30 mM SDS, 10 mM n-EM, pH 7.9, reveals a single mononuclear Cu^{II} species having a rhombically distorted environment ($g_x \neq g_y \neq g_z$; $A_x \neq A_y \neq A_z$). Examination of the perpendicular region (Figure 5a, 315–325 mT) reveals the presence of nitrogen superhyperfine coupling. Increased resolution was obtained through differentiation of the spectrum, and the high frequency noise was carefully removed with Fourier filtering (Hamming function) without distorting the original spectrum, Figure 5b. Expansion of the perpendicular (x, y) region reveals ^{63}Cu and ^{14}N hyperfine coupling. Each copper hyperfine resonance will be split into $2nI + 1$ ($I = 1$) resonances from coupling to a number (n) of magnetically equivalent nitrogen nuclei. These resonances will also have a characteristic intensity pattern, for example, coupling to four magnetically equivalent nitrogen nuclei will result in nine ^{14}N hyperfine resonances with an intensity pattern of (1:4:10:16:19:16:10:4:1). Computer simulation of both the first (Figure 5a) and second derivative (Figure 5b) spectra assuming a rhombic spin Hamiltonian (eq 1) and four magnetically equivalent nitrogen nuclei with the **g** and hyperfine (**A**(^{63}Cu and ^{14}N)) matrices given in Table 1

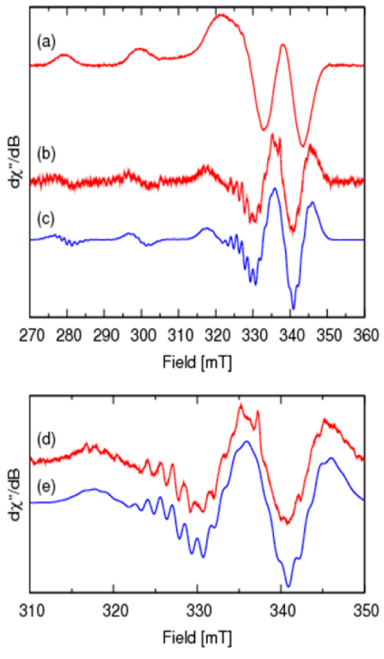

Figure 5. X-band (ν = 9.441882) EPR spectra of [Cu^{II}(NKB)$_2$] in 30 mM SDS, 10 mM n-EM, pH 7.9, measured at 140 K: (a) first derivative spectrum; (b) second derivative Fourier filtered spectrum; (c) computer simulation, see Table 1 and Table S1, Supporting Information, for spin Hamiltonian and line width parameters; (d,e) expansion of the perpendicular region of spectra b and c, respectively revealing the nitrogen superhyperfine coupling.

Table 1. Spin Hamiltonian Parameters for [Cu^{II}(NKB)$_2$]

g_x	2.040	$A_x(^{63}Cu)^a$	22.31	$A_x(^{14}N)^a$	13.70
g_y	2.047	$A_y(^{63}Cu)^a$	18.32	$A_y(^{14}N)^a$	13.85
g_z	2.179	$A_z(^{63}Cu)^a$	203.2	$A_z(^{14}N)^a$	13.07

^{a}Units 10^{-4} cm^{-1}.

yields the second derivative spectrum in blue (Figure 5c). Expansion of the perpendicular region of both the experimental (Figure 5d) and the simulated spectra (Figure 5e) highlights the ^{14}N superhyperfine coupling and the excellent agreement between the simulated (Figure 5e) and experimental spectra, confirming the presence of four ligating nitrogen atoms in the Cu^{II} ions coordination sphere. Plotting the $g_{\|}$ and $A_{\|}$ (^{63}Cu) for [Cu^{II}(NKB)$_2$] (Table 1) on the Blumberg–Peisach plots[46] confirms a [CuN_4] center and suggests the presence of a neutral species, which is consistent with the lack of a peak in the mass spectrum.

Copper-Binding Alters the Structure of NKB. NKB is similar to many other neuropeptides that interact with transmembrane receptors (such as GPCRs) in that it is unstructured in solution but adopts structure when bound to membranes or in membrane mimicking environments.[37,47] To assess the effect of copper-binding on NKB structure we used circular dichroism spectroscopy. The UV CD spectrum of apo-NKB in 30 mM SDS, 10 mM nEM, pH 7.9 (Figure 6) shows two negative peaks at 208 and 225 nm and a positive peak at 195 nm. These peaks are characteristic of an α-helical structure, which is consistent with previous structural studies and is thought to be a physiologically relevant state.[4,37,38] The addition of 0.5, 1.0, and 1.5 equiv of copper results in a loss of intensity of all peaks, and a plot of the absolute intensity of the negative peaks as a function of the copper equivalents added shows that copper addition beyond 0.5 equiv has little effect on the intensity (Figure 6B). In accord with the visible CD and electronic absorption spectroscopy, this confirms a stoichiometry of 1:2 Cu^{II}/NKB. It is likely that the loss of absolute intensity is because some helical structure needs to unwind in order to accommodate copper binding to His3 and the N-terminus. The formation of a weak negative band at

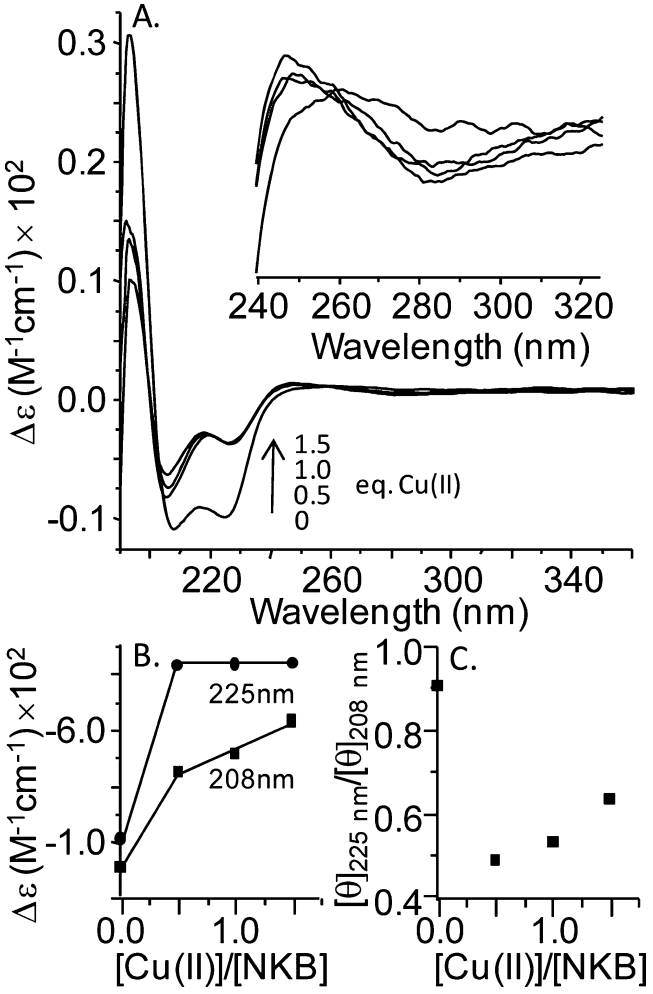

Figure 6. Cu^{II} titration of NKB monitored by UV circular dichroism spectroscopy. (A) The CD spectrum of NKB (108.5 mM, 30 mM SDS, 10 mM nEM, pH 7.9) was collected prior to the addition of copper (0 equiv of Cu^{II} spectrum) and after the addition of 0.5, 1.0, and 1.5 equiv of $CuCl_2$. Inset shows an expansion of the region between 240 and 325 nm. (B) The change in the absolute intensity of the peaks at 208 and 225 nm is plotted as a function of Cu^{II} equivalents added. This shows a plateau (225 nm) and a change in slope (208 nm) after 0.5 equiv of added Cu^{II}. (C) A plot of $[\theta]_{225nm}/[\theta]_{208nm}$ as a function of Cu^{II} equivalents added shows a decrease from 0.91 to 0.48 at 0.5 equiv of Cu^{II} added.

~284 nm (Figure 6, inset) is consistent with an amine−Cu^{II} charge transfer transition.[48] It is possible that this peak also arises from aromatic contributions from phenylalanine, which is responsible for transitions between 250 and 270 nm. The absence of any significant additional transitions in the 300−320 nm region suggests that amide−Cu^{II} coordination is not occurring.[48,24] Intriguingly, the loss of signal at 208 nm is less than the loss at 225 nm, and a plot of the CD signal ($[\theta]$) at these two wavelengths as a function of copper equivalents (Figure 6C) shows that the ratio drops from about 0.9 to about 0.5 at 0.5 equiv of Cu^{II}. The differential change to the peaks at 208 and 225 nm suggests that, along with loss of helix, the copper-bound peptide may adopt a 3_{10} helix. A 3_{10} helix has a $[\theta]_{225nm}/[\theta]_{208nm}$ ratio of approximately 0.4 compared with an α-helix that has a ratio near unity.[49] Addition of Cu^{II} to NKB results in a decrease in the ratio from an apo-NKB value of ~0.9 to ~0.48 in the presence of a stoichiometric amount of copper (Figure 6C). Additionally, loss of intensity at wavelengths <200 nm could be accounted for by an increase in irregular structure, which has a negative CD signal around 195 nm.

Copper Is Taken up by 1321N1 Astrocytoma Cells. We have shown that copper is able to bind to NKB, altering its structure and forming a binary complex, and a recent report has shown that dimerization of the neurotensin (8−13) peptide substantially reduced affinity for its receptor.[50] To determine whether copper-binding altered NKB's function, we assessed how intracellular calcium concentrations, $[Ca]_i$, changed in response to NKB and copper. As a model, we used the astrocyte cell line 1321N1 and initially confirmed the expression of the astrocyte marker, GFAP, along with the presence of the preferred NKB receptor, NK3-R, and NK1-R, the receptor preferred by SP (Figure 7A−C). NK3-R and NK1-

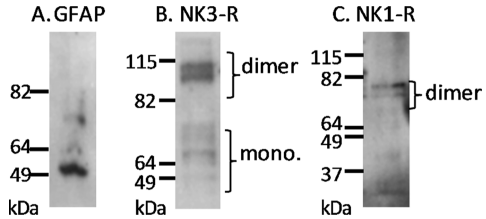

Figure 7. Western blot of astrocytoma (1321N1) cell lysates detects the presence of (A) glial fibrillary acidic protein (GFAP), (B) the neurokinin B receptor (NK3-R), and (C) the substance P receptor (NK1-R).

R appear as dimers, which has been observed previously.[51,52] We also confirmed that copper up to 50 μM had a negligible effect on astrocyte viability (Figure S4, Supporting Information).

First, we studied the effect of copper on calcium mobility in 1321N1 cells. After preparation of cell suspensions, copper (~0.6 μM) was added, and the Fura2 excitation at 340 and 380 nm was monitored with emission at 510 nm. Figure 8A shows that the addition of copper results in an immediate decrease in the Fl_{340}/Fl_{380} ratio. The decrease is due to quenching of the fluorescence of the calcium-bound Fura2 because the fluorescence after excitation at 340 nm (Ca-bound Fura2) is quenched and the fluorescence after excitation at 380 nm (apo-Fura2) remains unchanged (Figure 8B). A similar effect was not seen when zinc was added (data not shown), but other metals such as manganese are known to quench Fura2 fluorescence.[53] Analogously to Mn-quenching, copper must enter the cells and quench the Ca−Fura2 complex; an identical effect has previously been observed for pulmonary arterial endothelial cells.[54] This shows that copper is readily taken up into 1321N1 cells, which supports previous studies showing that astrocytes accumulate copper.[55] No change in the fluorescence ratio is observed after copper addition suggesting that copper is not causing release of calcium from intracellular stores, because it is likely that any increase in $[Ca^{II}]_i$ would result in at least partial recovery of the Fl_{340}/Fl_{380} ratio. Addition of excess calcium to the extracellular buffer results in an immediate increase in the Fl_{340}/Fl_{380} ratio, which is due to recovery of the fluorescence after excitation at 340 nm (i.e., due to recovery of Ca−Fura2 fluorescence, Figure 8A,B). The recovery is due to the influx of calcium into the cell, presumably as a result of the copper-induced opening of plasma membrane calcium channels. To exclude the possibility that the 1321N1 astrocytes have a

dx.doi.org/10.1021/cn4000988 | ACS Chem. Neurosci. 2013, 4, 1371−1381

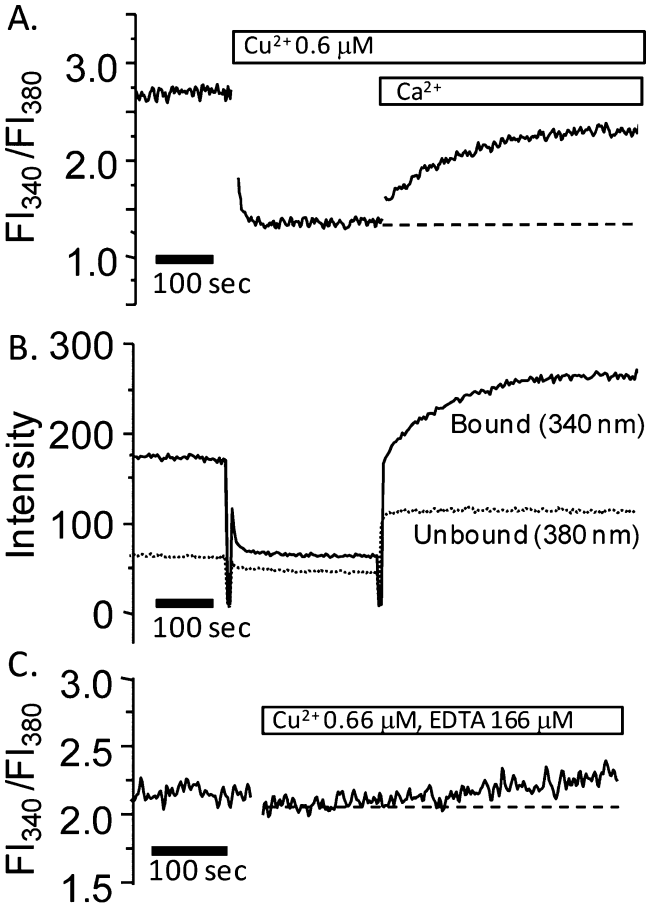

Figure 8. Copper-dependent quenching of Ca^{II}-bound Fura2 fluorescence in 1321N1 astrocytoma cells. Cells were suspended in 10 mM HEPES, pH 7.6, with NaCl (130 mM), KCl (4.7 mM), $MgSO_4$ (1.2 mM), NaH_2PO_4 (1.2 mM), and glucose (11.5 mM) with no added calcium and monitored at room temperature. (A) The ratio of the fura2 fluorescence at 510 nm after excitation at 340 and 380 nm (Fl_{340}/Fl_{380}) is plotted as a function of time. After stabilization, the addition of $CuCl_2$ (0.66 μM) results in a decrease in the ratio, which can be partially reversed after the addition of excess Ca^{II} to the extracellular media. (B) The absorbance at 510 nm after excitation at 340 nm (Ca^{II}-bound Fura2, solid line) and 380 nm (unbound Fura2, dotted line) shows that copper addition only results in a decrease in the fluorescence after excitation at 340 nm. (C). Addition of $CuCl_2$ (0.66 μM) in the presence of excess EDTA (166 μM) shows no decrease in Fl_{340}/Fl_{380}.

significant basal concentration of open calcium channels, we added calcium to the medium in the absence of copper. This did not result in any increase in the Fl_{340}/Fl_{380} ratio (Figure S5A, Supporting Information). It is unlikely that copper is affecting store-operated calcium channels because the recovery after copper quenching was still apparent in the presence of the lanthanide Gd^{III} at concentrations known to inhibit these calcium channels (Figure S5B,C, Supporting Information).[56−58] The mechanism underlying the copper-induced influx of calcium was not investigated further and remains unclear, although voltage-opened channels have been implicated[54] and calcium influx via copper-sensitive NMDA receptors remains a possibility.[59] The ability of copper to open plasma membrane channels is likely to lead to a potentially dangerous disruption of intracellular calcium levels if copper uptake is not controlled, so we next investigated whether chelation can limit copper-induced Fura2 quenching by adding copper in the presence of the high-affinity chelator ethylenediaminetetraacetic acid (EDTA, log $K_1 \approx 19$). Figure 8C shows that the quenching is suppressed in the presence of excess EDTA.

Binding of Copper by NKB Inhibits Uptake of the Metal into 1321N1 Astrocytoma Cells. Having assessed the impact of copper on the astrocytes, we next determined whether copper can affect NKB's ability to trigger intracellular calcium changes and whether NKB can act as a chelator and limit uptake of the metal. Analogously to the effect of EDTA, we can monitor the inhibition of copper uptake by the absence of copper-induced quenching of Ca−Fura2 fluorescence. Because copper was able to open plasma membrane channels, it was necessary to conduct all experiments with NKB in the absence of Ca^{II} in the medium. NKB alone resulted in a mild increase in the Fl_{340}/Fl_{380} fluorescence ratio (Figure 9A) that is reasonably sustained. This suggests that NKB elicits only a small increase in cytosolic calcium after release from the ER. This result is atypical in that GPCR agonists usually elicit an initial transient Ca^{II} release. Due to the atypical nature, we tested cells at different passage numbers, bought in a new cell batch from the ECCC, and conducted experiments on adherent cells maintained on a coverslip inserted into a fluorescence cuvette, yet all displayed the same response to NKB. The result may reflect a poor efficiency of IP_3 generation in these cells or a poor spatial coupling between the site of IP_3 generation and the IP_3-sensitive receptors.[60] NK3-R is also thought to traffic to the nucleus, and the immunoblot (Figure 7B) does not differentiate between surface and intracellular protein.[52] Furthermore, despite these astrocytes expressing NK3-R, it may not be predominantly linked to release of Ca^{II} from the ER. Indeed, recent work has shown that in dorsal root ganglia neurons, SP activation of NK1-R does not produce substantial releases of Ca^{II} but is instead linked to an alternative pathway that releases reactive oxygen species from mitochondria.[61] Attenuation of the Ca^{II} increase in response to NKB when in the presence of the high-affinity NK3-R specific antagonist SB222200 indicates that we are observing interaction of NKB with NK3-R in the 1321N1 cells (Jones et al., unpublished data). When $[Cu^{II}(NKB)_2]$ is added the change in the Fl_{340}/Fl_{380} is not significantly different from that observed with NKB alone (Figure 9B), although we note that the initial increase in Fl_{340}/Fl_{380} is slightly greater with the complex. The lack of copper-dependent quenching but a similar rise in $[Ca^{II}]_i$ to that with NKB alone suggests that NKB can limit uptake of copper into the cells while not altering its own ability to change $[Ca^{II}]_i$. NKB is still binding Cu^{II} because no quenching due to "free" copper uptake is observed, but the addition of Cu^{II} beyond stoichiometry (>0.5 equiv) results in a decrease in Fl_{340}/Fl_{380} (Figure 9B). This result further supports the formation of a $[Cu^{II}(NKB)_2]$ binary complex. To investigate the lack of copper-dependent Ca−Fura2 quenching further, we used a peptide derived from the prion protein, PrP(107−114) (sequence Ac-TNMKHMAG). This peptide has known Cu^{II} binding properties and has a moderate, micromolar to nanomolar copper affinity and thus represents a copper-binding site that is more physiologically relevant than EDTA.[62,63] When Cu^{II}PrP(107−114), in the same buffer as $[Cu^{II}(NKB)_2]$, is added to the Fura2-loaded astrocytes, there is an immediate decrease in the Fl_{340}/Fl_{380} ratio with no recovery of the Fl_{340}/Fl_{380} ratio until Ca^{II} is added to the medium (Figure 9C). This is similar to that observed with copper alone (Figure 8A). Further, the tachykinin peptide SP, which has no copper

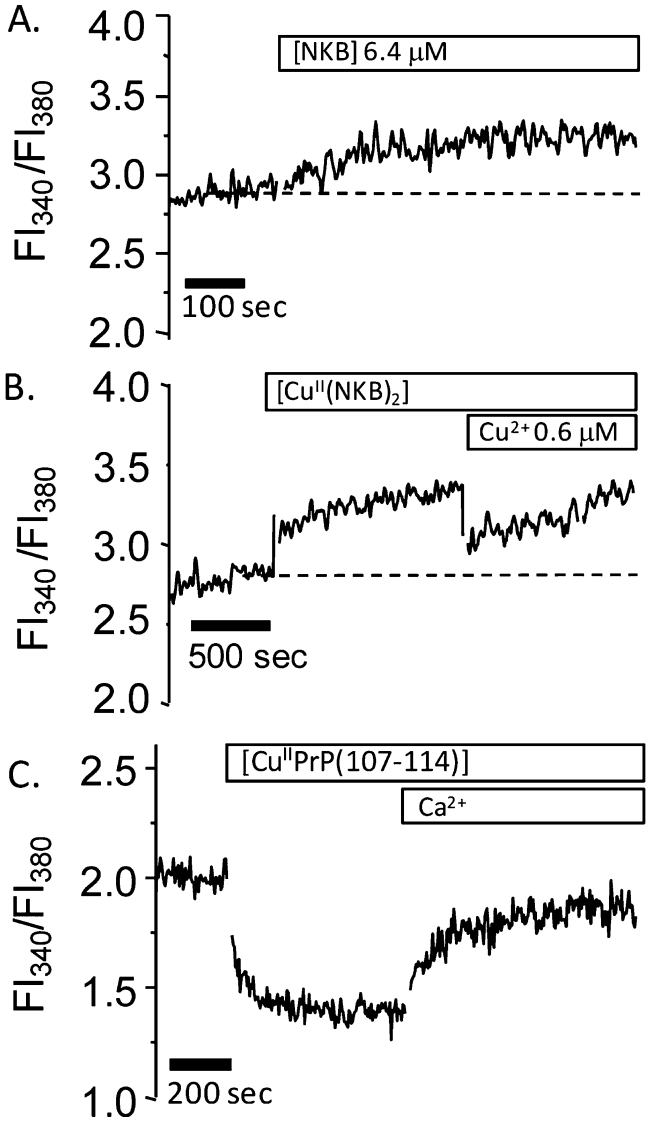

Figure 9. NKB can limit cellular uptake of Cu^{II}. The 1321N1 astrocytoma cells were suspended in 10 mM HEPES, pH 7.6, with NaCl (130 mM), KCl (4.7 mM), $MgSO_4$ (1.2 mM), NaH_2PO_4 (1.2 mM), and glucose (11.5 mM) with no added calcium. (A) Addition of NKB (6.4 μM) to the cell suspension increases the Fl_{340}/Fl_{380} ratio. (B) Addition of $[Cu^{II}(NKB)_2]$ ([NKB] = 6.4 μM, $[Cu^{II}]$ = 3.0 μM) to the cell suspension increases the Fl_{340}/Fl_{380} ratio similarly to that seen in panel A. Addition of additional copper (3.2 μM) causes quenching of fluorescence. (C) Addition of $[Cu^{II}PrP(107-114)]$ ($[PrP(107-114)]$ = 2.98 μM, $[Cu^{II}]$ = 1.38 μM) to the cell suspension results in an immediate decrease in the Fl_{340}/Fl_{380} ratio, which can be partially recovered by the addition of excess Ca^{II} to the cell medium.

binding ability at pH 7.6, did not inhibit the copper-induced quenching of Ca−Fura2 (Figure S1B, Supporting Information).

DISCUSSION

The stoichiometry of 1:2 Cu/NKB that we have determined from CD (Figures 1 and 6) and electronic absorption (Figure 2) titrations and EPR spectroscopy (Figure 5) indicates formation of a neutral mononuclear Cu^{II} species ($[Cu^{II}(NKB)_2]$), which is highly unusual for an ATCUN-containing peptide. In contrast, the binding of Ni^{II} results in a 1:1 complex with an absorption maxima at 420 nm (Figure 3), suggesting that Ni^{II} is bound in a square-planar, diamagnetic environment, and both the Ni^{II} stoichiometry and geometry are entirely consistent with binding by an ATCUN motif. [34] It therefore appears that this peptide is perfectly able to bind Ni^{II} via the ATCUN motif but with copper a binary structure ($[Cu^{II}(NKB)_2]$) is preferred. The binding of Cu^{II} by NKB involves the His3 imidazole side chain, and evidence from near-UV CD suggests that there is N-terminal amine coordination but, unexpectedly, not amide coordination. Binding to amide nitrogens causes changes to the α- and β-protons of nearby amino acids; however no specific change (either broadening or chemical shift changes) in these protons was seen in the NMR (Figure S2, Supporting Information) supporting the conclusion that main-chain coordination is not occurring. EPR analysis indicates that the Cu^{II} ions' equatorial coordination sphere involves four nitrogen ligands, and our data suggests that two molecules of NKB coordinate to copper forming a mononuclear Cu^{II} center, where each NKB chain donates a histidine imidazole and an N-terminal nitrogen $\{2N_{Im}, 2N_{amine}\}$ to fulfill the four nitrogen equatorial coordination sphere.

The ability of copper to bind to NKB and alter its structure suggested that copper may alter the binding of NKB to its preferred NK3 receptor. In contrast though, we observed that $[Cu^{II}(NKB)_2]$ was similar to metal-free NKB in the ability to induce intracellular calcium release. This suggests that, like metal-free NKB, $[Cu^{II}(NKB)_2]$ can interact with the cell surface and translocate to the correct receptor. It is somewhat surprising that copper did not affect NKB function; however, the interaction of NKB with NK3-R, as with any of the tachykinins, is thought to be mediated by the conserved FxGLM-NH_2 C-terminal motif, and we have established that copper binds to N-terminal amino acids. Our results suggest that the binding of copper to the N-terminus does not alter the C-terminal region enough to limit receptor binding, despite structural changes and the formation of $[Cu^{II}(NKB)_2]$. It is not unprecedented that changes to the N-terminal region have little effect on NKB activity, because a modified, disulfide-bridged $[Cys_2-Cys_5]$ NKB peptide was shown to be almost as potent as wild-type NKB. [64] However, selectivity may be affected, and it is possible that copper binding has modified the receptor preference and $[Cu^{II}(NKB)_2]$ can bind to other tachykinin receptors, such as NK1-R.

An interesting result from this work is that the binding of copper by NKB can suppress uptake of the metal into astrocytes. The lack of copper-dependent quenching of the Ca−Fura2 fluorescence in the presence of NKB indicates that the metal is not entering the cytoplasm. Only copper directly bound to NKB was prevented from being taken up, because copper in excess of stoichiometry (i.e., >0.5 equiv) was able to quench fluorescence. In contrast, a copper-binding peptide derived from the prion protein, PrP(107−114), which binds copper as a monomer and via histidine and backbone nitrogen/carbonyl atoms[62] is unable to limit copper uptake. Copper is primarily taken up into cells via the high-affinity pump Ctr1,[65] and we speculate that $Cu^{II}PrP(107-114)$ readily transfers copper to Ctr1 (or the reductases that reduce Cu^{II} for transfer by Ctr1) but $[Cu^{II}(NKB)_2]$ does not. $[Cu^{II}PrP(104-117)]$ is a soluble monomeric complex, whereas $[Cu^{II}(NKB)_2]$ is a membrane-bound binary complex, and this may explain the inability of $[Cu^{II}(NKB)_2]$ to readily lose the metal. Unsurprisingly, the tachykinin substance P did not limit uptake of the metal ion into astrocytes, due to the inability to bind copper. This result may further distinguish a role for NKB within the tachykinin family.

Rather than copper acting in the synapse to modulate NKB function, the work described here suggests that NKB can help modify copper activity in the brain. Given the ability of copper to enter cells and subsequently open calcium channels, it is possible that copper released from neurons may act as a signaling molecule to modify calcium levels in adjacent cells, and this may also help explain why copper is released in a "free" or unbound state.[59] Being able to control the activity of extracellular "free" copper is vital because the metal ion in this state can be involved in the generation of reactive oxygen species and can bind to a range of synaptic components. Several copper-binding proteins are prevalent on the surface of neurons and astrocytes and in the synapse, including prions and Aβ-peptides.[66] These proteins have similar histidine imidazole and nitrogen ligands for copper but contain more sites along with quite diverse binding modes and variable stoichiometry.[25,63,67−69] Proteins such as prions and Aβ-peptides have also been implicated in brain copper homeostasis, but having a neuropeptide (and as such a transient molecule) such as NKB present to bind and control copper usage and uptake confers an added level of spatial and temporal control of synaptic copper activity. In neurodegenerative disorders such as AD, where a change in both copper and calcium homeostasis is well established, it is possible that the excess extracellular copper leads to the disruption of calcium levels.[70] Given the links we have shown between copper, NKB, and calcium, we predict that any loss of NKB (potentially as a result of loss of NKB expressing cells) may be a contributory element in the dysregulation of copper and calcium observed in AD.

CONCLUSIONS

In summary, we have utilized a range of spectroscopic techniques (CD, UV/vis and EPR) to show that NKB can bind Cu^{II} in an unusual neutral binary complex $[Cu^{II}(NKB)_2]$ that utilizes two N-terminal amine and two imidazole nitrogen ligands (from each molecule of NKB) and the binding substantially alters the structure of the peptide. Despite altering the structure, copper does not impede the ability of neurokinin B to trigger intracellular calcium release in 1321N1 astrocytoma cells. Further, we have shown that copper can enter the cells and subsequently open plasma membrane calcium channels but when bound to neurokinin B copper ion uptake is inhibited. Our data suggest a novel role for neurokinin B in protecting cells against copper-induced calcium changes and implicate the peptide in synaptic copper homeostasis.

METHODS

Materials. Neurokinin B (DMHDFFVGLM-NH_2) was purchased from Auspep (Melbourne, Australia), substance P (RPKPQQFFGLM-NH_2) was purchased from Sigma Aldrich (Castle Hill, Sydney, Australia), and PrP(107−114) (Ac-TNMKHMAG) was synthesized by Proteomics International (Perth, WA, Australia). All peptides were >95% purity (assessed by mass spectrometry and NMR analysis) and were used without further purification. Antibodies for immunoblotting were anti-NK3-R (polyclonal, Lifespan Technologies, Seattle, WA, USA) and anti-NK1-R (polyclonal), anti-GFAP (monoclonal) and anti-GAPDH, all from Sigma Aldrich, Castle Hill, Sydney, Australia. Secondary antibodies were HRP-conjugated goat anti-rabbit or anti-mouse (Sigma Aldrich, Castle Hill, Sydney, Australia). Unless specified, all other chemicals and materials were obtained from Sigma Aldrich (Castle Hill, Sydney, Australia). Milli-Q purified (>18 MΩ) water was used for all experiments.

Metal Ion Titrations. Stock (0.5 M) solutions of Cu^{II} and Ni^{II} were prepared as $CuCl_2{\cdot}2H_2O$ and $NiCl_2{\cdot}2H_2O$ in water and diluted to working solutions on the day of use. Lyophilized peptides were dissolved in 30 mM SDS, 10 mM *n*-ethylmorpholine, pH 7.9, or in 100% DMSO followed by dilution into 10 mM *n*-ethylmorpholine (n-EM). n-EM has previously been shown to have limited copper binding ability.[71] The concentration of NKB or SP was determined by using the absorbance at 259 nm and an extinction coefficient of phenylalanine (190 $M^{-1}cm^{-1}$ × number of phenylalanines), and this correlated well with the concentration determined after weighing the peptide and using the supplier's recommendation that the lyophilized peptide contained 25% water. UV/visible absorption spectroscopy (Perkin-Elmer U-3100) was used to monitor metal binding. Spectra throughout this study were processed using Microsoft Excel and plotted using Origin software.

Circular Dichroism (CD) Spectroscopy. CD spectra were acquired at 25 °C on a Jasco J810 spectophotometer. In the visible region (400−800 nm), a 10 mm path length cell was used with sampling every 1 nm, and 20 scans were acquired for each sample. The baseline (apo-NKB) was subtracted from each spectrum collected. In the UV region, a 1 mm path length cuvette was used to acquire spectra over the range 190−290 nm with sampling every 0.5 nm, and 3 scans were averaged.

Nuclear Magnetic Resonance (NMR) Spectroscopy. NMR spectra were obtained on a Bruker Avance 600 MHz spectrometer equipped with a 5 mm TXI BBI probe (Bruker Biospin, Germany). Samples were prepared in 10% D_2O and 30 mM SDS-d_{25} and the pH adjusted to 7.6 using HCl or NaOH. The residual water signal was suppressed using either a low power presaturation pulse or a W5 watergate sequence.[72] Proton spectra were acquired over a 12 ppm spectral width, with 64000 complex data points. Data were acquired and processed using Bruker TopSpin software running on a Linux workstation. The one-dimensional spectra were processed using a $\pi/2$ shifted sine-squared window function.

Electron Paramagnetic Resonance (EPR) Spectroscopy. Continuous wave EPR spectra at ∼9.4 GHz (X-Band) were obtained on a Bruker Elexsys E580 spectrometer operated with Bruker Xepr software. Spectra were obtained using either a super high-Q or optical cavity (X-band). The microwave frequency and magnetic field were calibrated with a Bruker microwave frequency counter and a Bruker ER036TM teslameter. A nitrogen gas flow through system in conjunction with a Eurotherm B-VT-2000 variable temperature controller provided stable temperatures of ∼140 K. Spectra were routinely baseline corrected using polynomial functions, differentiated, and smoothed using Fourier filtering available in the Xepr software to remove high frequency noise. Care was taken to not distort the EPR spectrum, by comparing the filtered and experimental spectra. Analysis of the EPR spectra was performed using the XSophe−Sophe−XeprView (version 1.1.4) computer simulation software suite running on a Linux (Mandriva 2010.2) workstation. Computer simulation of the randomly oriented frozen solution spectra employed a rhombic spin Hamiltonian (eq 1), naturally abundant isotopes, and a **g**- and **A**-strain line shape function.

$$\mathbf{H} = \beta\mathbf{B}\cdot g\cdot\mathbf{S} + \sum_{i=\mathrm{Cu,N}} \mathbf{S}\cdot A_i\cdot\mathbf{I}_i - g_{ni}\beta_{ni}\mathbf{B}\cdot\mathbf{I}_i \quad (1)$$

Matrix diagonalization was employed for the determination of the resonant field positions arising from the electron Zeeman and copper hyperfine interactions, and the nitrogen superhyperfine interactions were treated with perturbation theory.[73]

Liquid Chromatography Mass Spectrometry (LC-MS) Analysis. LC-MS analysis was performed on a nanoAquity UPLC (Waters Corp., Milford, MA, USA) linked to a Xevo QToF mass spectrometer from Waters (Micromass,UK). The mass spectrometer was operated in positive ESI mode with a capillary voltage of 3.5 kV, cone voltage of 40 V, source temperature of 80 °C, and mass ranges of 250−3000 Da. One microliter of sample was loaded onto a nanoAquity C18 BEH130 column (1.7 μm, 75 μm × 250 mm) and then eluted from the column using a binary gradient program at a flow rate of 0.3 μL/min: mobile phase A was 0.1% formic acid in water, and mobile phase B was 0.1% formic acid in acetonitrile. The nano-UPLC gradient was as follows: 0 min, 97:3 A/B; 1 min, 97:3 A/B; 30 min, 60:40 A/B; 40 min, 60:40 A/

B; 50 min, 5:95 A/B; 65 min, 5:95; 75 min, 97:3. Samples of NKB for MS analysis were prepared in 10 mM n-EM, pH7.4, 30 mM SDS. Spectral process and elemental analysis of peaks was undertaken using MassLynx software (Waters Corp. Milford, MA, USA).

Cell Culture. The 1321N1 astrocytoma cells were obtained from the European Cell Culture Collective (Sigma Aldrich, Castle Hill, Sydney, Australia). Cells were cultured in DMEM (Gibco) supplemented with 10% fetal calf serum, 10 units/mL penicillin, and 10 μg/mL streptomycin and incubated at 37 °C in a 5% CO_2 humidified incubator. Cells were regularly passaged at 70−80% confluency and were discarded at passage 10.

Calcium Assays. Changes in the concentration of intracellular calcium ($[Ca]_i$) was monitored using the calcium-binding fluorophore Fura2. To load with Fura2, cells were grown to ∼80% confluency in a T25 or T75 flask, washed with PBS, and collected into 2 mL of calcium-free HEPES buffer, pH 7.6 (HEPES, 10 mM; NaCl, 130 mM; KCl, 4.7 mM; $MgSO_4$, 1.2 mM; NaH_2PO_4, 1.2 mM; glucose, 11.5 mM). After collection, the cells were incubated for 30 min with 1 μM Fura2 AM LeakRes prepared in cell culture grade DMSO (working concentration, Sigma Aldrich, Castle Hill, Sydney, Australia), washed twice in HEPES buffer, and then left at room temperature for 40 min to allow hydrolysis of the acetomethoxy ester bond. Fluorescence spectra of cells ($\sim 1 \times 10^6$) were acquired on a Perkin-Elmer LS50B spectrometer using the ratiometric monitoring available in the Perkin-Elmer software (FL Winlab). The excitation wavelengths were set at 340 nm (Ca-bound Fura2) and 380 nm (Ca-free Fura2), and the emission wavelength was 510 nm. The fluorescence was allowed to settle prior to addition of any compounds. The spectra are plotted and shown as 340 nm/380 nm ratios. All fluorescence experiments were conducted at room temperature (∼22 °C).

Western Blots. The 1321N1 cells were immunoblotted for the presence of the NKB receptor (NK3-R), the SP receptor (NK1-R), and the astrocyte specific glial fibrillary acidic protein (GFAP). The cells were grown in a T25 flask, washed, and collected in 2 mL of cold phosphate-buffered saline (PBS). The collected cells were then incubated for 30 min in NP40 lysis buffer (NP40, 1%; Tris, 20 mM; NaCl, 137 mM; glycerol, 10%; pH 8) containing a protease inhibitor cocktail (Sigma Aldrich, Castle Hill, Sydney, Australia). Approximately 20 μg of protein was loaded onto a 12.5% acrylamide gel for sodium dodecyl sulfate electrophoresis alongside prestained standards (Invitrogen). After electrophoresis, the proteins were transferred to a PVDF membrane (at 4 °C, 100 V), and then the membrane was blocked in 5% milk powder in 0.1% tween-20 (TBS-T) (1 h at 4 °C). The membrane was then incubated overnight in the primary antibodies (anti-NK3-R, 1/1000; anti-NK1-R, 1/1000, anti-GFAP 1/5000) added to 5% milk/TBS-T. After incubation, the membrane was washed in TBS-T and then incubated for 1 h in the appropriate HRP-conjugated secondary antibody (1/20000) in 5% milk/TBS-T. The membrane was extensively washed in TBS-T prior to adding the chemiluminescent substrate (SuperSignal West Femto maximum sensitivity substrate, Thermo Scientific, IL, USA). X-ray film (CL-Xposure, Thermo Scientific) was exposed to the membrane and then manually developed using Kodak GBx developer and fixer (Sigma Aldrich, Castle Hill, Sydney, Australia).

■ ASSOCIATED CONTENT

Supporting Information

Additional tables and figures as described in the text. This material is available free of charge via the Internet at http://pubs.acs.org.

■ AUTHOR INFORMATION

Corresponding Author

*E-mail: c.jones@uws.edu.au. Phone: +61 2 9685 9908.

Author Contributions

D.R., G.R.H. and C.E.J. designed experiments, analyzed the data, and wrote the paper. E.M. and L.H. conducted experiments.

Funding

UWS is thanked for financial support.

Notes

The authors declare no competing financial interest.

■ ACKNOWLEDGMENTS

Project students James Lindsay and Shyama Williamson are thanked for undertaking initial experiments. Professor Tom Millar (UWS) is thanked for useful discussions and advice and his support, Prof. Janice Aldrich-Wright (UWS) is thanked for access to a CD spectrometer, and Allan Torres is thanked for NMR assistance.

■ ABBREVIATIONS

Aβ, amyloid beta; AD, Alzheimer's disease; CD, circular dichroism; ER, endoplasmic reticulum; EPR, electron paramagnetic resonance; GPCRs, G protein-coupled receptors; IP_3, inositol triphosphate; LC-MS, liquid chromatography−mass spectrometry; n-EM, n-ethylmorpholine; NKA, neurokinin A; NKB, neurokinin B; SP, substance P; TBS-T, tris-buffered saline−0.1% tween 20

■ REFERENCES

(1) Almeida, T. A., Rojo, J., Nieto, P. M., Pinto, F. M., Hernandez, M., Martin, J. D., and Candenas, M. L. (2004) Tachykinins and tachykinin receptors: Structure and activity relationships. *Curr. Med. Chem. 11*, 2045−2081.

(2) Pantaleo, N., Chadwick, W., Park, S. S., Wang, L., Zhou, Y., Martin, B., and Maudsley, S. (2010) The mammalian tachykinin ligand-receptor system: An emerging target for central neurological disorders. *CNS Neurol. Disord. Drug Targets 9*, 627−635.

(3) Macdonald, S. G., Dumas, J. J., and Boyd, N. D. (1996) Chemical cross-linking of the substance P (NK-1) receptor to the alpha subunits of the G proteins Gq and G11. *Biochemistry 35*, 2909−2916.

(4) Ganjiwale, A. D., Rao, G. S., and Cowsik, S. M. (2011) Molecular modeling of neurokinin B and tachykinin NK receptor complex. *J. Chem. Inf. Model. 51*, 2932−2938.

(5) Marriott, I. (2004) The role of tachykinins in central nervous system inflammatory responses. *Front. Biosci. 9*, 2153−2165.

(6) Topaloglu, A. K., Reimann, F., Guclu, M., Yalin, A. S., Kotan, L. D., Porter, K. M., Serin, A., Mungan, N. O., Cook, J. R., Ozbek, M. N., Imamoglu, S., Akalin, N. S., Yuksel, B., O'Rahilly, S., and Semple, R. K. (2009) TAC3 and TACR3 mutations in familial hypogonadotropic hypogonadism reveal a key role for Neurokinin B in the central control of reproduction. *Nat. Genet. 41*, 354−358.

(7) Navarro, V. M., Ruiz-Pino, F., Sanchez-Garrido, M. A., Garcia-Galiano, D., Hobbs, S. J., Manfredi-Lozano, M., Leon, S., Sangiao-Alvarellos, S., Castellano, J. M., Clifton, D. K., Pinilla, L., Steiner, R. A., and Tena-Sempere, M. (2012) Role of neurokinin B in the control of female puberty and its modulation by metabolic status. *J. Neurosci. 32*, 2388−2397.

(8) Beaujouan, J. C., Torrens, Y., Saffroy, M., Kemel, M. L., and Glowinski, J. (2004) A 25 year adventure in the field of tachykinins. *Peptides 25*, 339−357.

(9) Merchenthaler, I., Maderdrut, J. L., O'Harte, F., and Conlon, J. M. (1992) Localization of neurokinin B in the central nervous system of the rat. *Peptides 13*, 815−829.

(10) Marksteiner, J., Saria, A., and Krause, J. E. (1992) Comparative distribution of neurokinin B-, substance P- and enkephalin-like immunoreactivities and neurokinin B messenger RNA in the basal forebrain of the rat: evidence for neurochemical compartmentation. *Neuroscience 51*, 107−120.

(11) Mileusnic, D., Lee, J. M., Magnuson, D. J., Hejna, M. J., Krause, J. E., Lorens, J. B., and Lorens, S. A. (1999) Neurokinin-3 receptor distribution in rat and human brain: an immunohistochemical study. *Neuroscience 89*, 1269−1290.

(12) Griebel, G., and Beeske, S. (2012) Is there still a future for neurokinin 3 receptor antagonists as potential drugs for the treatment of psychiatric diseases? *Pharmacol. Ther. 133*, 116−123.
(13) Spooren, W., Riemer, C., and Meltzer, H. (2005) Opinion: NK3 receptor antagonists: the next generation of antipsychotics? *Nat. Rev. Drug Discovery 4*, 967−975.
(14) Kowall, N. W., Quigley, B. J., Jr., Krause, J. E., Lu, F., Kosofsky, B. E., and Ferrante, R. J. (1993) Substance P and substance P receptor histochemistry in human neurodegenerative diseases. *Regul. Pept. 46*, 174−185.
(15) Yankner, B. A., Duffy, L. K., and Kirschner, D. A. (1990) Neurotrophic and neurotoxic effects of amyloid beta protein: Reversal by tachykinin neuropeptides. *Science 250*, 279−282.
(16) Marolda, R., Ciotti, M. T., Matrone, C., Possenti, R., Calissano, P., Cavallaro, S., and Severini, C. (2012) Substance P activates ADAM9 mRNA expression and induces alpha-secretase-mediated amyloid precursor protein cleavage. *Neuropharmacology 62*, 1954−1963.
(17) Mantha, A. K., Moorthy, K., Cowsik, S. M., and Baquer, N. Z. (2006) Neuroprotective role of neurokinin B (NKB) on beta-amyloid (25−35) induced toxicity in aging rat brain synaptosomes: involvement in oxidative stress and excitotoxicity. *Biogerontology 7*, 1−17.
(18) Kowall, N. W., Beal, M. F., Busciglio, J., Duffy, L. K., and Yankner, B. A. (1991) An in vivo model for the neurodegenerative effects of beta amyloid and protection by substance P. *Proc. Natl. Acad. Sci. U.S.A. 88*, 7247−7251.
(19) Flashner, E., Raviv, U., and Friedler, A. (2011) The effect of tachykinin neuropeptides on amyloid beta aggregation. *Biochem. Biophys. Res. Commun. 407*, 13−17.
(20) Bush, A. I. (2013) The metal theory of Alzheimer's disease. *J. Alzheimer's Dis. 33*, S277−281.
(21) Craddock, T. J., Tuszynski, J. A., Chopra, D., Casey, N., Goldstein, L. E., Hameroff, S. R., and Tanzi, R. E. (2012) The zinc dyshomeostasis hypothesis of Alzheimer's disease. *PLoS One 7*, No. e33552.
(22) Bush, A. I., Pettingell, W. H., Multhaup, G., d Paradis, M., Vonsattel, J. P., Gusella, J. F., Beyreuther, K., Masters, C. L., and Tanzi, R. E. (1994) Rapid induction of Alzheimer A beta amyloid formation by zinc. *Science 265*, 1464−1467.
(23) Minicozzi, V., Stellato, F., Comai, M., Serra, M. D., Potrich, C., Meyer-Klaucke, W., and Morante, S. (2008) Identifying the minimal copper- and zinc-binding site sequence in amyloid-beta peptides. *J. Biol. Chem. 283*, 10784−10792.
(24) Syme, C. D., Nadal, R. C., Rigby, S. E. J., and Viles, J. H. (2004) Copper binding to the amyloid-β (Aβ) peptide associated with Alzheimer's disease - Folding, coordination geometry, pH dependence, stoichiometry, and affinity of Aβ-(1−28): Insights from a range of complementary spectroscopic techniques. *J. Biol. Chem. 279*, 18169−18177.
(25) Drew, S. C., Noble, C. J., Masters, C. L., Hanson, G. R., and Barnham, K. J. (2009) Pleomorphic copper coordination by Alzheimer's disease amyloid-beta peptide. *J. Am. Chem. Soc. 131*, 1195−1207.
(26) Drew, S. C., Masters, C. L., and Barnham, K. J. (2009) Alanine-2 carbonyl is an oxygen ligand in Cu2+ coordination of Alzheimer's disease amyloid-beta peptide–relevance to N-terminally truncated forms. *J. Am. Chem. Soc. 131*, 8760−8761.
(27) Sarell, C. J., Syme, C. D., Rigby, S. E., and Viles, J. H. (2009) Copper(II) binding to amyloid-beta fibrils of Alzheimer's disease reveals a picomolar affinity: stoichiometry and coordination geometry are independent of Abeta oligomeric form. *Biochemistry 48*, 4388−4402.
(28) Kardos, J., Kovács, I., Hajós, F., Kálmán, M., and Simonyi, M. (1989) Nerve endings from rat brain tissue release copper upon depolarization. A possible role in regulating neuronal excitability. *Neurosci. Lett. 103*, 139−144.
(29) Hopt, A., Korte, S., Fink, H., Panne, U., Niessner, R., Jahn, R., Kretzchmar, H., and Herms, J. (2003) Methods for studying synaptosomal copper release. *J. Neurosci. Methods 128*, 159−172.
(30) Peters, C., Munoz, B., Sepulveda, F. J., Urrutia, J., Quiroz, M., Luza, S., De Ferrari, G. V., Aguayo, L. G., and Opazo, C. (2011) Biphasic effects of copper on neurotransmission in rat hippocampal neurons. *J. Neurochem. 119*, 78−88.
(31) Adlard, P. A., Cherny, R. A., Finkelstein, D. I., Gautier, E., Robb, E., Cortes, M., Volitakis, I., Liu, X., Smith, J. P., Perez, K., Laughton, K., Li, Q. X., Charman, S. A., Nicolazzo, J. A., Wilkins, S., Deleva, K., Lynch, T., Kok, G., Ritchie, C. W., Tanzi, R. E., Cappai, R., Masters, C. L., Barnham, K. J., and Bush, A. I. (2008) Rapid restoration of cognition in Alzheimer's transgenic mice with 8-hydroxy quinoline analogs is associated with decreased interstitial Abeta. *Neuron 59*, 43−55.
(32) Pietruszka, M., Jankowska, E., Kowalik-Jankowska, T., Szewczuk, Z., and Smuzynska, M. (2011) Complexation abilities of neuropeptide gamma toward copper(II) ions and products of metal-catalyzed oxidation. *Inorg. Chem. 50*, 7489−7499.
(33) Kowalik-Jankowska, T., Jankowska, E., Szewczuk, Z., and Kasprzykowski, F. (2010) Coordination abilities of neurokinin A and its derivative and products of metal-catalyzed oxidation. *J. Inorg. Biochem. 104*, 831−842.
(34) Harford, C., and Sarkar, B. (1997) Amino terminal Cu(II)- and Ni(II)-binding (ATCUN) motif of proteins and peptides: Metal binding, DNA cleavage, and other properties. *Acc. Chem. Res. 30*, 123−130.
(35) Sadler, P. J., Tucker, A., and Viles, J. H. (1994) Involvement of a lysine residue in the N-terminal Ni2+ and Cu2+ binding site of serum albumins. Comparison with Co2+, Cd2+ and Al3+. *Eur. J. Biochem. 220*, 193−200.
(36) Biran, J., Palevitch, O., Ben-Dor, S., and Levavi-Sivan, B. (2012) Neurokinin Bs and neurokinin B receptors in zebrafish-potential role in controlling fish reproduction. *Proc. Natl. Acad. Sci. U.S.A. 109*, 10269−10274.
(37) Whitehead, T. L., McNair, S. D., Hadden, C. E., Young, J. K., and Hicks, R. P. (1998) Membrane-induced secondary structures of neuropeptides: A comparison of the solution conformations adopted by agonists and antagonists of the mammalian tachykinin NK1 receptor. *J. Med. Chem. 41*, 1497−1506.
(38) Mantha, A. K., Chandrashekar, I. R., Baquer, N. Z., and Cowsik, S. M. (2004) Three dimensional structure of mammalian tachykinin peptide neurokinin B bound to lipid micelles. *J. Biomol. Struct. Dyn. 22*, 137−148.
(39) Tsangaris, J. M., and Martin, R. B. (1970) Visible circular dichroism of copper(II) complexes of amino acids and peptides. *J. Am. Chem. Soc. 92*, 4255−4260.
(40) At pH 7.9 (Figure 2A), there is a distinct rise in the absorbance above 0.5 equiv of Cu^{II} and shift of the band to slightly lower wavelength. The absence of these observations in the CD titrations indicates the presence of achiral Cu^{II} species, most likely copper hydroxide. A fine copper hydroxide precipitate produces Rayleigh light scattering, which would account for these observations. The presence of copper hydroxide is also apparent in the EPR spectra of solutions containing Cu/NKB 2:1 at pH 7.9, Figure S3, Supporting Information.
(41) Klewpatinond, M., and Viles, J. H. (2007) Empirical rules for rationalising visible circular dichroism of Cu^{2+} and Ni^{2+} histidine complexes: Applications to the prion protein. *FEBS Lett. 581*, 1430−1434.
(42) Jones, C. E., Taylor, P. J., McEwan, A. G., and Hanson, G. R. (2006) Spectroscopic characterization of copper(II) binding to the immunosuppressive drug mycophenolic acid. *J. Am. Chem. Soc. 128*, 9378−9386.
(43) van den Brenk, A. L., Tyndall, J. D., Cusack, R. M., Jones, A., Fairlie, D. P., Gahan, L. R., and Hanson, G. R. (2004) Formation of mononuclear and chloro-bridged binuclear copper(II) complexes of patellamide D, a naturally occurring cyclic peptide: influence of anion and solvent. *J. Inorg. Biochem. 98*, 1857−1866.

(44) Comba, P., Dovalil, N., Gahan, L. R., Haberhauer, G., Hanson, G. R., Noble, C. J., Seibold, B., and Vadivelu, P. (2012) Cu(II) coordination chemistry of patellamide derivatives: possible biological functions of cyclic pseudopeptides. *Chemistry 18*, 2578−2590.
(45) Since electrospray mass spectroscopy relies heavily on protonation of basic side chains and the N-terminus to generate ions, coordination of histidine and the N-terminus by Cu^{II} would make formation of protonated, charged species difficult and accounts for our inability to observe substantial copper-bound peaks in the mass spectroscopic data.
(46) Peisach, J., and Blumberg, W. E. (1974) Structural implications derived from the analysis of electron paramagnetic resonance spectra of natural and artificial copper proteins. *Arch. Biochem. Biophys. 165*, 691−708.
(47) Schwyzer, R. (1995) In search of the 'bio-active conformation'–is it induced by the target cell membrane? *J. Mol. Recognit. 8*, 3−8.
(48) Muller, D., Decock-Le Reverend, B., and Sarkar, B. (1984) Studies of copper(II) binding to glycylglycyl-L-tyrosine-N-methyl amide, a peptide mimicking the NH2-terminal copper(II)-binding site of dog serum albumin by analytical potentiometry, spectrophotometry, CD, and NMR spectroscopy. *J. Inorg. Biochem. 21*, 215−226.
(49) Toniolo, C., Polese, A., Formaggio, F., Crisma, M., and Kamphuis, J. (1996) Circular dichroism spectrum of a peptide 3_{10}-helix. *J. Am. Chem. Soc. 118*, 2744−2745.
(50) Richter, S., Ramenda, T., Bergmann, R., Kniess, T., Steinbach, J., Pietzsch, J., and Wuest, F. (2010) Synthesis of neurotensin(8−13)-phosphopeptide heterodimers via click chemistry. *Bioorg. Med. Chem. Lett. 20*, 3306−3309.
(51) Jensen, D., Zhang, Z., and Flynn, F. W. (2008) Trafficking of tachykinin neurokinin 3 receptor to nuclei of neurons in the paraventricular nucleus of the hypothalamus following osmotic challenge. *Neuroscience 155*, 308−316.
(52) Sladek, C. D., Stevens, W., Levinson, S. R., Song, Z., Jensen, D. D., and Flynn, F. W. (2011) Characterization of nuclear neurokinin 3 receptor expression in rat brain. *Neuroscience 196*, 35−48.
(53) Hellwig, N., Albrecht, N., Harteneck, C., Schultz, G., and Schaefer, M. (2005) Homo- and heteromeric assembly of TRPV channel subunits. *J. Cell Sci. 118*, 917−928.
(54) Demura, Y., Ishizaki, T., Ameshima, S., Okamura, S., Hayashi, T., Matsukawa, S., and Miyamori, I. (1998) The activation of nitric oxide synthase by copper ion is mediated by intracellular Ca2+ mobilization in human pulmonary arterial endothelial cells. *Br. J. Pharmacol. 125*, 1180−1187.
(55) Scheiber, I. F., Mercer, J. F., and Dringen, R. (2010) Copper accumulation by cultured astrocytes. *Neurochem. Int. 56*, 451−460.
(56) Putney, J. W. (2010) Pharmacology of store-operated calcium channels. *Mol. Interventions 10*, 209−218.
(57) Ahmmed, G. U., Mehta, D., Vogel, S., Holinstat, M., Paria, B. C., Tiruppathi, C., and Malik, A. B. (2004) Protein kinase Calpha phosphorylates the TRPC1 channel and regulates store-operated Ca2+ entry in endothelial cells. *J. Biol. Chem. 279*, 20941−20949.
(58) Bird, G. S., DeHaven, W. I., Smyth, J. T., and Putney, J. W., Jr. (2008) Methods for studying store-operated calcium entry. *Methods 46*, 204−212.
(59) Schlief, M. L., Craig, A. M., and Gitlin, J. D. (2005) NMDA receptor activation mediates copper homeostasis in hippocampal neurons. *J. Neurosci. 25*, 239−246.
(60) Delmas, P., Wanaverbecq, N., Abogadie, F. C., Mistry, M., and Brown, D. A. (2002) Signaling microdomains define the specificity of receptor-mediated InsP(3) pathways in neurons. *Neuron 34*, 209−220.
(61) Linley, J. E., Ooi, L., Pettinger, L., Kirton, H., Boyle, J. P., Peers, C., and Gamper, N. (2012) Reactive oxygen species are second messengers of neurokinin signaling in peripheral sensory neurons. *Proc. Natl. Acad. Sci. U.S.A. 109*, E1578−1586.
(62) Jones, C. E., Abdelraheim, S. R., Brown, D. R., and Viles, J. H. (2004) Preferential Cu^{2+} coordination by His^{96} and His^{111} induces β-sheet formation in the unstructured amyloidogenic region of the prion protein. *J. Biol. Chem. 279*, 32018−32027.
(63) Walter, E. D., Stevens, D. J., Spevacek, A. R., Visconte, M. P., Dei Rossi, A., and Millhauser, G. L. (2009) Copper binding extrinsic to the octarepeat region in the prion protein. *Curr. Protein Pept. Sci. 10*, 529−535.
(64) Lavielle, S., Chassaing, G., Besseyre, J., Marquet, A., Bergstrom, L., Beaujouan, J. C., Torrens, Y., and Glowinski, J. (1986) A cyclic analogue selective for the NKB specific binding site on rat brain synaptosomes. *Eur. J. Pharmacol. 128*, 283−285.
(65) Banci, L., Bertini, I., Cantini, F., and Ciofi-Baffoni, S. (2010) Cellular copper distribution: a mechanistic systems biology approach. *Cell. Mol. Life Sci. 67*, 2563−2589.
(66) Badrick, A. C., and Jones, C. E. (2010) Use, control and metallic interplay of copper in the brain, in *Horizons in Neuroscience Research* (Costa, A., and Villalba, E., Eds.), pp 95−117, Nova Science Publishers, Hauppauge, NY.
(67) Stellato, F., Spevacek, A., Proux, O., Minicozzi, V., Millhauser, G., and Morante, S. (2011) Zinc modulates copper coordination mode in prion protein octa-repeat subdomains. *Eur. Biophys. J. 40*, 1259−1270.
(68) Emwas, A. H., Al-Talla, Z. A., Guo, X., Al-Ghamdi, S., and Al-Masri, H. T. (2013) Utilizing NMR and EPR spectroscopy to probe the role of copper in prion diseases. *Magn. Reson. Chem. 51*, 255−268.
(69) Ghosh, C., and Dey, S. G. (2013) Ligand-field and ligand-binding analysis of the active site of copper-bound Abeta associated with Alzheimer's disease. *Inorg. Chem. 52*, 1318−1327.
(70) Schlief, M. L., West, T., Craig, A. M., Holtzman, D. M., and Gitlin, J. D. (2006) Role of the Menkes copper-transporting ATPase in NMDA receptor-mediated neuronal toxicity. *Proc. Natl. Acad. Sci. U.S.A. 103*, 14919−14924.
(71) Garnett, A. P., and Viles, J. H. (2003) Copper binding to the octarepeats of the prion protein - Affinity, specificity, folding, and cooperativity: Insights from circular dichroism. *J. Biol. Chem. 278*, 6795−6802.
(72) Liu, M. L., Mao, X. A., Ye, C. H., Huang, H., Nicholson, J. K., and Lindon, J. C. (1998) Improved WATERGATE pulse sequences for solvent suppression in NMR spectroscopy. *J. Magn. Reson. 132*, 125−129.
(73) Hanson, G. R., Gates, K. E., Noble, C. J., Griffin, M., Mitchell, A., and Benson, S. (2004) XSophe-Sophe-XeprView. A computer simulation software suite (v. 1.1.3) for the analysis of continuous wave EPR spectra. *J. Inorg. Biochem. 98*, 903−916.